LABORATORY WAVE FORCES ON VERTICAL CYLINDERS

by

John H. Nath, Professor, Ocean Engineering, Oregon State University

Ming-Kuang Hsu, Graduate Student, Ocean Engineering, Oregon State University

Robert T. Hudspeth, Professor, Ocean Engineering, Oregon State University

Jerry Dummer, Civil Engineer, Naval Civil Engineering Laboratory, Port Hueneme, CA

Abstract

Local wave forces were measured on vertical cylinders with three surface roughnesses -- smooth, sand roughened (ε/D = .023) and artificially marine roughened (ε/D = .09). Two diameters of smooth cylinders were tested -- 12 3/4 inches and 8 5/8 inches. A data analysis method, based on phase shift and maximum force, for determining the force transfer coefficients, is introduced and compared with results from least squares techniques. The phase shift method has promise for reducing the scatter that is inherent in the results from force experiments in waves. It simplifies the determination of C_d and C_m and it clarifies the relative importance between the inertia term and the drag term in the Morison equation.

INTRODUCTION

Experiments were performed at the Oregon State University O. H. Hinsdale Wave Research Laboratory (WRL) in relatively large laboratory waves on three types of cylinders. The first was a smooth, nominally 12-inch diameter cylinder which had an actual outside diameter of 12 3/4 inches. It will be referred to herein as the VSMC12. It was instrumented for local and total forces in the in-line and transverse directions with respect to the wave travel direction. It also had local pressure transducers arranged on the periphery of the local force transducer. This paper reports on some aspects of the in-line local force measurements only.

A vertical smooth, nominally 8-inch diameter cylinder was also tested with an actual outside diameter of 8 5/8 inches. It will be referred to herein as the VSMC8. It was instrumented for in-line and

transverse local forces only at the same level in the water column as the VSMC12. Again, only the in-line forces will be reported on for this cylinder and those that are described next.

A vertical, sand roughened cylinder and artificially marine roughened cylinder were also instrumented and tested in the same way as the VSMC8. They are referred to as the VSRC.02 and the AMRC. The sand grains were angular and uniform in size such that k/D = .023 where k is the sand size and D is the cylinder diameter. Both cylinders had a nominal diameter of 8 inches and the AMRC had an equivalent k/D = .09, which was determined from circumferential measurements.

The testing range in waves was from $0.4 < K < 25.5$ and $0.16\times10^5 < R < 2.7\times10^5$, where K is the Keulegan Carpenter number and R is the Reynolds number. The cylinders were also tested in random waves but the results from that testing will not be reported herein. The 8-inch diameter cylinders were also towed at steady speed in the horizontal orientation in the Reynolds number range of from $0.3\times10^5 < R < 7\times10^5$ (3, 4).

The objective of the 12-inch diameter cylinder testing was to produce a high quality set of information that can be used to study several aspects of the wave force question. At this stage, drag and inertia coefficients have been calculated from local force measurements for the periodic wave condition. It was intended that this test be strongly dependent on both the drag and inertia forces. Drag dominance could not be achieved at the K obtainable in the WRL. According to Dean (1) if $0.25 < R < 4$, both C_d and C_m (the drag and inertia coefficients) are important and experiments will be well conditioned to determine both C_d and C_m. Herein, R will be termed the Dean number. It is defined in (1) and it can be shown that $R = 0.088\,K$ for linear wave theory, which indicates that the data will be well-conditioned for both C_d and C_m when $2.8 < K < 45$. One would expect inertia forces to dominate for $K \lesssim 2.8$ and drag forces to dominate for $K \gtrsim 45$.

The 8-inch diameter cylinder work was part of another study on smooth, sand roughened and artificially marine roughened cylinders for investigating the effects of marine roughened cylinders on the wave forces (3,4). The study was done on both horizontal and vertical cylinders but this paper only utilizes the vertical cylinder information in conjunction with the steady state tow results for the horizontal cylinders.

In the course of the work on the VSMC12, it was observed that the maximum forces occurred closer in phase to the zero upcrossing condition of the water surface than to the wave crest. This indicated that the force was more heavily influenced by the inertia term than the drag term than was anticipated. This prompted a study of the effects of the two terms in the Morison equation on the phase and the maximum force coefficient. This adjunct study led to an alternative way of considering wave forces on a vertical cylinder. The basic premise is not new but this may be a first time that a complete analysis of C_d and C_m is based on the maximum force coefficient, C_μ, and the phase shift between the water surface and the total force measurement, ϕ.

The results from the tests on the smooth cylinders showed that the magnitude of the forces was almost completely dominated by the inertia effects within the range $K < 9$. The phase showed no influence whatever from the drag term for $K < 4$. In addition, the magnitude of the force was almost completely dominated by the drag term for approximately $300 < K$. This indicates a much stronger and important influence for the inertia coefficient than anticipated. These ranges on K were changed considerably for the roughened cylinders.

Also shown here is the importance of the steady drag coefficient in laboratory wave studies as a limiting condition at high values of K. The possibility arises of connecting two extremes of laboratory information to provide drag and inertia coefficients that more accurately predict the *maximum* forces than the coefficients obtained from least square methods. It may become possible to predict with at least fair accuracy field forces from waves, using only laboratory information from waves such as those produced at the WRL.

It should be emphasized that this paper is speculative in nature. The results presented are tentative. More knowledge is needed on best analysis techniques to reduce scatter. Time constraints made it not possible to investigate all the different methods of analyses for best results. However, the subject matter on the basic analysis may be of enough importance to express them now with the intent to refine certain procedures in the future. The ideas expressed here may be helpful to other researchers to be able to place their experiment in a better known relation with respect to the range that exists between laboratory and field conditions.

ANALYSIS

The Morison equation estimates the wave force per unit length, $F(t)$, acting on a vertical cylinder as

$$F = C_d \frac{D\rho}{2} u|u| + C_m \frac{\pi D^2}{4} \rho \dot{u} \tag{1}$$

where C_d is the drag coefficient, C_m is the inertia coefficient (1 + added mass coefficient), D is the cylinder diameter, ρ is the mass density of the water, u is the horizontal water particle velocity, and and $\dot{u}$ is the temporal water particle acceleration. It is sometimes convenient to assume linear wave theory where

$$u = u_\mu \cos(kx-\omega t) \tag{2}$$

where u_μ is the maximum, or amplitude, of the horizontal velocity, k is the wave number ($= 2\pi/L$, with L the wave length) and ω is the radian wave frequency ($= 2\pi/T$, with T the wave period). In this paper the subscript, μ, will be used to indicate maximum value. Herein, we set x=o and shift t so that

$$u = u_\mu \cos\omega t \tag{3}$$

Equation (1) is non-dimensionalized by dividing through by $D\rho u_\mu^2/2$, setting $\theta=\omega t$, and other manipulations to

$$F = C_d \cos\theta|\cos\theta| - \frac{\pi^2}{K} C_m \sin\theta \tag{4}$$

where K is the Keulegan-Carpenter number ($= u_\mu T/D$).

The first term in Eq. 4 can be expressed with the first two terms of a Fourier series, such that

$$\cos\theta|\cos\theta| = \frac{8}{3\pi}(\cos\theta - \frac{1}{5}\cos 3\theta) \tag{5}$$

If the second term of Eq. 5 is dropped, the linearization results

$$\cos\theta|\cos\theta| \approx .85\cos\theta \tag{6}$$

which is the same result achieved with the Lorentz linearization principle of equivalent work. Thus, a linear form of the non-dimensional Morison equation can be approximated by

$$F = .85\,C_d\cos\theta - \frac{\pi^2}{K}\,C_m\sin\theta\ . \tag{7}$$

Thus,

$$F_\mu = C_\mu = [(.85\,C_d)^2 + (\frac{\pi^2}{K}\,C_m)^2]^{1/2} \tag{8}$$

and the phase between the wave crest and the maximum force is

$$\phi = \tan^{-1}\,(-\frac{\pi^2\,C_m}{.85\,K\,C_d})\ . \tag{9}$$

From Eq. 9, we have

$$C_m = \frac{.85\,K\,C_d}{\pi^2}\tan\,(-\phi) \tag{10}$$

and by substituting into Eq. 8, we obtain

$$C_d = \frac{C_\mu\cos\phi}{.85} \tag{11}$$

by using the identity $\cos\phi = 1/(1 + \tan^2\phi)^{1/2}$. Thus, Eq. 10 can be further simplified to

$$C_m = \frac{K\,C_\mu\sin(-\phi)}{\pi^2}\ . \tag{12}$$

From Eq. 4 the maximum value of the force is expressed as

$$F_\mu = C_\mu = C_d\cos\phi|\cos\phi| - \frac{\pi^2}{K}\,C_m\sin\phi \tag{13}$$

and as K gets very large when the wave period gets large,

$$\lim_{K\to\infty}\ C_\mu = C_{ds} \tag{14}$$

where C_{ds} is the drag coefficient for steady flow. However, the linearized form, Eq. 7, yields

$$\lim_{K\to\infty}\ C_\mu = .85\,C_{ds} \neq C_{ds}, \tag{15}$$

which illustrates one weakness of the linearization procedure.

As K gets very small, the phase shift should approach -90°, (or $-\pi/2$), so the limit of C_m in Eq. 12 is undefined, but we would expect $C_m \to 2.0$ as K gets small. Since $\phi \to -90°$ for small K

$$\lim_{K\to o}\ C_d = 0 \tag{16}$$

from Eq. 11.

One need not linearize the Morison equation. If we consider that the maximum force occurs at some time between the zero upcrossing of the wave and the wave crest (in the time domain), in that phase quadrant

$$F = C_d\cos^2\theta - \frac{\pi^2}{K}\,C_m\sin\theta\ . \tag{17}$$

Then the maximum force occurs when $dF/d\theta = 0$, which is the phase shift, ϕ, between the wave crest and F_μ. Thus,

$$\phi = \sin^{-1}\,(-\frac{\pi^2 C_m}{2K\,C_d})\ . \tag{18}$$

By using $\cos^2\theta = 1-\sin^2\theta$ and by substitution of Eq. 18 into Eq. 17,

$$C_\mu = C_d\,(1 + \gamma^2) \tag{19}$$

and

$$\phi = \sin^{-1}\gamma \tag{20}$$

where

$$\gamma = \frac{-\pi^2 C_m}{2K\,C_d} \quad . \tag{21}$$

As $K \to \infty$, $\gamma \to 0$, $\phi \to 0$ and $C_\mu \to C_{ds}$. As $K \to 0$, $\gamma \to \infty$, $C_\mu \to \infty$ and ϕ oscillates, which does not correspond to reality. For the force transfer coefficients,

$$C_d = C_\mu(1 + \gamma^2)^{-1} \tag{22}$$

or

$$C_d = C_\mu\,(1 + \sin^2\phi)^{-1} \tag{23}$$

and

$$C_m = \frac{2KC_d}{\pi^2}\sin(-\phi). \tag{24}$$

Now, consider the phase at which either the drag or inertia term dominates the maximum force, F_μ. Since this concept is rather approximate consider the linearized form, Eqs. 7, 8 and 9. Let C_μ be influenced only, say, 4% by the inertia term. Then

$$\left[1 + \left(\frac{\pi^2 C_m}{.85K\,C_d}\right)^2\right]^{1/2} = 1.04 \tag{25}$$

and

$$\frac{\pi^2 C_m}{.85K\,C_d} = .286 = \tan(-\phi) \tag{26}$$

So,

$$\phi = -16^\circ \quad . \tag{27}$$

Likewise, if C_μ is to be influenced, say, only 4% by the drag term, then

$$\phi = -74^\circ \quad . \tag{28}$$

(Herein a negative phase shift indicates the maximum force precedes the wave crest in time.) These limits will be useful later when the test results are considered.

EXPERIMENTS AND DATA ANALYSIS

Experimental work was done in the O. H. Hinsdale Wave Research Laboratory at Oregon State University (WRL). The overall length of the wave flume is 340 ft. The depth at the wave board is 14.5 ft. with an additional 3.5 ft. for freeboard. The water depth reduces to 11.5 ft. in 40 ft. just downwave from the wave board. In the evanescent region near the wave board, the water motion is not the same as a purely propagating wave. The test length of the flume is considered to be free from the shoaling effects of the rise of the bottom, free of the wave board evanescent region and in the region upwave from the toe of the beach. Thus, about 129 ft. constitutes the length in which tests can be performed free of these deleterious effects.

The location of the test cylinders was 136 ft. downwave from the wave board, which was 92 ft. within the acceptable test region. Good, repeatable waves can be produced with this facility, ranging from a high frequency of 1.0 Hz to a low of about .12 Hz. For these tests, the wave frequencies ranged from .4 Hz to .17 Hz which were digitized at the rate of 256 readings per wave period. Information was recorded digitally in real time on a PDP 11 computer. These data were later analyzed on the OSU main-frame computer. Currents were measured with Marsh-McBirney current meters directly opposite the cylinder location so that the currents should be in phase with the water surface elevation at the cylinder. The water surface elevation was measured directly above the current meter measurements at the cylinder location.

Steady tow tests were made with nominally 8-inch diameter horizontal cylinders, which are reported in (3). For the nominally 8-inch diameter cylinders, data were recorded for four wave periods after the first transient waves reached the cylinder. Of these four waves,

three peak-to-peak waves were later defined for analysis by least squares techniques. The results from the three waves were averaged for reporting herein. For the nominal 12-inch diameter cylinder, eight waves were recorded of which seven were analyzed and averaged.

The phase shift between the water surface and the force measurement was determined in three ways. The first was by averaging the phase shift between the upcrossings and downcrossings of the force and water profile measurements. The second was by averaging the phase shift between the crest of the wave and the maximum force. The third method was by using cross correlation methods on the entire test record. In retrospect, the logical phase to be measured is the second one -- from the wave crest to the maximum force. However, the least scatter occurs by using the cross correlation method. Some aspects of all three methods will be reported. However, because of time constraints and because the least scatter results from the cross correlation methods, they will be emphasized to some degree.

RESULTS

Smooth Cylinders

The phase shift results, calculated from the cross correlation method for the 8 and 12 inch diamter cylinders, are shown in Fig. 1. The phase has been normalized so that $\hat{\phi} = \phi/-90°$. Although two completely different test cylinder constructions were used with their own distinctive calibrations (2,3) and the tests were done in different years, it can be seen that the VSMC8 results mesh very well with the VSMC12 results. Unfortunately, K only extends to about 26. However, for illustrative purposes at least, a straight line has been drawn tangent to the curve. This type of plot was also done, at the last minute while this paper was in production, for the phase shift to the force peak, F_μ. There was a little more scatter but essentially the same result was obtained as for Fig. 1.

According to Eqs. 27 and 28, drag effects should predominate when $\hat{\phi} < .18$, which occurs on the dashed line at about K = 300. Inertia effects should predominate when $\hat{\phi} > .82$, which occurs at about K = 9. These two limits are shown as dotted lines on Fig. 1

The phase plot is not dependent on any specific theory. The only analysis was the cross correlation computation. The data points in Fig. 1 are purely the result of laboratory measurements. Figure 1 illustrates the values of K when the force becomes more in phase with the acceleration of the particle motion (high $\hat{\phi}$), or more in phase with the velocity (small $\hat{\phi}$). It is useful as a direct measure of the influence of the velocity or acceleration terms in the Morison equation. From that equation, one then derives limits on ϕ for drag and inertia predominance, from which the K values are then determined from the experimental plot.

Another revealing plot is that for C_μ, which is Fig. 2. Again, the results from the 12-inch and 8-inch diameter cylinders are superimposed. At very high K, the value for $C_{ds} = .5$ is indicated, which is the average value obtained for the 8-inch diameter horizontal cylinder towed up to Reynolds number of about 6×10^5. The limiting value for K at which steady state results should occur is unknown. However, the values for C_μ appear to be closely clustered around the straight line indicated and their lowest value is about .8. With respect to Fig. 2, there is not much distance between $C_\mu = .8$ and $C_\mu = C_{ds} = .5$, so that it seems to be conservative to assign the $C_\mu = .5$ condition at $K \gtrsim 500$.

For the smooth cylinder, the plots of $\hat{\phi}$ and C_μ are independent of the period parameter, $\beta (= R/K)$. Thus, they are independent of Reynolds number. It should be noted that $6130 > \beta > 14{,}700$ and (5) shows that for oscillating flow C_m is constant at $C_m = 2.0$ and C_d seems to approach a limiting value for $\beta >$ from about 5000 to 8000. Thus, one would expect ϕ and C_μ to be independent of R for these values of β. We found that such was not necessarily the case for roughened cylinders.

How C_μ varies in the range $25 < K < 500$ needs to be established by measurements in the laboratory and in the field. For purposes of this paper, to illustrate a proposed procedure only, the variation of C_μ in this range of K is assumed as the curved dashed line in Fig. 2.

Values for C_d and C_m for the linear and nonlinear cases were calculated from the lines fit by eye for Figs. 1 and 2 using Eqs. 11, 12, 23 and 24. These theoretical curves for C_d and C_m were plotted in Fig. 3 and compared to the values obtained from a least squares analysis. The 12-inch cylinder results are shown as small circles and the 8-inch cylinder results are the filled-in circles. The 12-inch circle least

squares analysis was based on the measured kinematics whereas the 8-inch cylinder results were based on stream function kinematics.

The results show that the 12-inch cylinder C_m calculations are in close agreement between the least squares calculation and the phase shift method. The 8-inch cylinder C_m's are considerably lower, which is probably due to the different kinematics used in the analyses. Another possibility that comes to mind is that the Reynolds number for the smaller cylinder is lower. However, we witness a regular decrease in C_m for the smaller cylinder for all $K < 12$. Sarpkaya's results for oscillatory flow show a constant $C_m = 2.0$ for $K < 5$ and sharply defined large differences in C_m, depending on R (or β), for $K < 8$. However, for the Reynolds number range (or β) in this study, Sarpkaya's data show $C_m \approx 2.0$ within the entire range of K. Our lowest β values were near the highest values in (5).

The drag coefficient trend seems to favor the linearized value for the range of K in these experiments. There is more scatter for the 8-inch cylinder but it is mostly bounded by the linearized "theoretical" C_d. The values for the 12-inch cylinder closely follow the linearized case for $K < 7$ except for one point. One's first thought might be that the scatter demonstrated could be organized with respect to R. This was tried at a larger scale than Fig. 3, to no avail. No reasonable contours of Reynolds number could be seen except that very generally higher Reynolds numbers were obtained at higher Keulegan-Carpenter numbers.

Rough Cylinders

The VSRC.02 data for phase shift was analyzed in three different ways -- by cross correlation methods, by observing and recording the average phase between the zero upcrossings and downcrossings and by observing and recording the phase between the crest of the wave and the maximum force. The results are shown in Fig. 4. They show that the up and downcrossing method is more influenced by the acceleration effects in the wave. The peak-to-peak method is more influenced by the drag, or velocity dependent, features of the waves and that the cross correlation method is truly an averaging, or smoothing technique. There is more scatter in the peak-to-peak method and the differences show more clearly where $K > 12$.

The analysis for the SRC.02 and the AMRC used their effective diameter based on circumferential measurements. The $\hat{\phi}$ and C_μ values are shown in Figs. 5 and 6. Using the effective diameter, the averaged C_{ds} was 1.0 for both cylinders. The results for the VSRC.02 did not have much spread with respect to β, but the much rougher VAMRC did. The values of β were therefore not noted for the VSRC.02, but they are indicated as shown for the AMRC. The results from constant values of β are better disciplined for C_μ than for $\hat{\phi}$. The effects of the rougher AMRC are seen in both Figs. 5 and 6.

The results for the combined VSMC8 and VSMC12 are indicated in Figs. 5 and 6 with dashed lines. The VSRC.02 results are superimposed on those for the VSMC for $K \lesssim 10$, and they clearly deviate from the VSMC results toward their respective C_{ds} values at $K \approx 20$.

The lower β values may be interpreted as those where the wave length is much larger than the cylinder diameter. If lower β is combined with relatively high R, meaning that K must also be large, then the conditions at sea are approached. Figure 6 shows that C_μ (therefore C_d) will be lower for high β values, approaching the limiting value of the smooth cylinder.

CONCLUSIONS

The phase shift method of analysis shows promise of being a powerful tool for analyzing and comparing in-line forces for vertical cylinders in waves. Its use for other cylinder orientations is not known, but will be explored in the near future.

Forces on vertical smooth cylinders in waves are completely dominated by (in phase with) the acceleration components of the wave when $K < 4$. The amplitude of the force is dominated by the acceleration components when $K \lesssim 9$. The wave force on a vertical smooth cylinder may continue to be influenced significantly by acceleration components up to $K \approx 200$, 300, or more. More data are needed to establish that limit.

The maximum force coefficient for a sand roughened cylinder (with $k/D = .02$) behaves very much like a smooth cylinder if $K < 10$. However, the phase shift, $\hat{\phi}$, is quite different for $K < 4$. Thus, at lower K values the roughness has more influence on $\hat{\phi}$ than on C_μ.

ACKNOWLEDGEMENTS

The 12-inch cylinder data were collected for a project jointly funded by the Naval Civil Engineering Laboratory and Minerals Management Service, contract N62474-82-C-8295. The 8-inch cylinder data were collected from aspects of different projects funded by the National Science Foundation, Grant No. CEE-8310732, the OSU Sea Grant Program, NA81AA-D-00086, and the American Petroleum Institute, PRAC Project 80-31.

REFERENCES

1. Dean, R. G., "Methodology for Evaluating Suitability of Wave and Wave Force Data for Determining Drag and Inertia Coefficients," Proceedings of the International Conference Behavior of Offshore Structures (BOSS '76), Trondheim, Norway, Vol. 2, August 1976.

2. Hudspeth, R. T. and Nath, J. H., "High Reynolds Number Wave Force Investigation in a Wave Flume, Volume I," Final report to Naval Civil Engineering Laboratory and Minerals Management Service, Ocean Engineering Program, Dept. of Civil Engineering, Oregon State University, February 1984.

3. Nath, J. H., "Heavily Roughened Horizontal Cylinders in Waves," BOSS '82 Conference Proceedings, MIT, August 1982.

4. Nath, J. H., "Vertical vs. Horizontal Cylinders in Waves," ASCE Conference Proceedings on Pipelines in Adverse Environments II, San Diego, CA, November 14-16, 1983.

5. Sarpkaya, T. and Isaacson, M., Mecnanics of Wave Forces on Offshore Structures, Van Nostrand Reinhold Co., 1981.

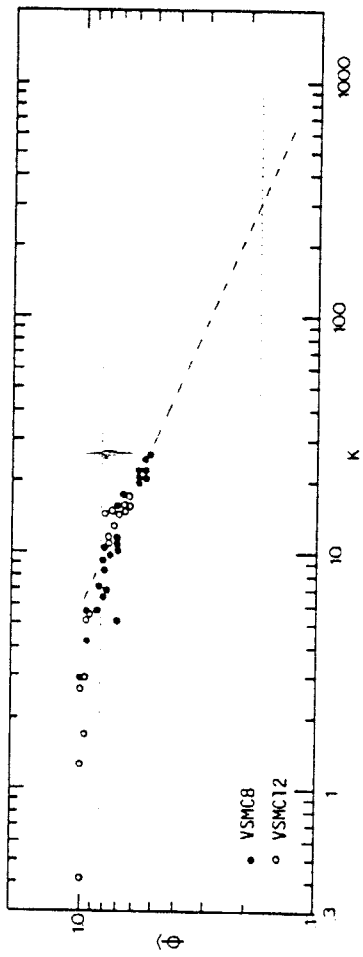

Fig. 1 Normalized phase shift for smooth vertical cylinders tested, by cross correlation method

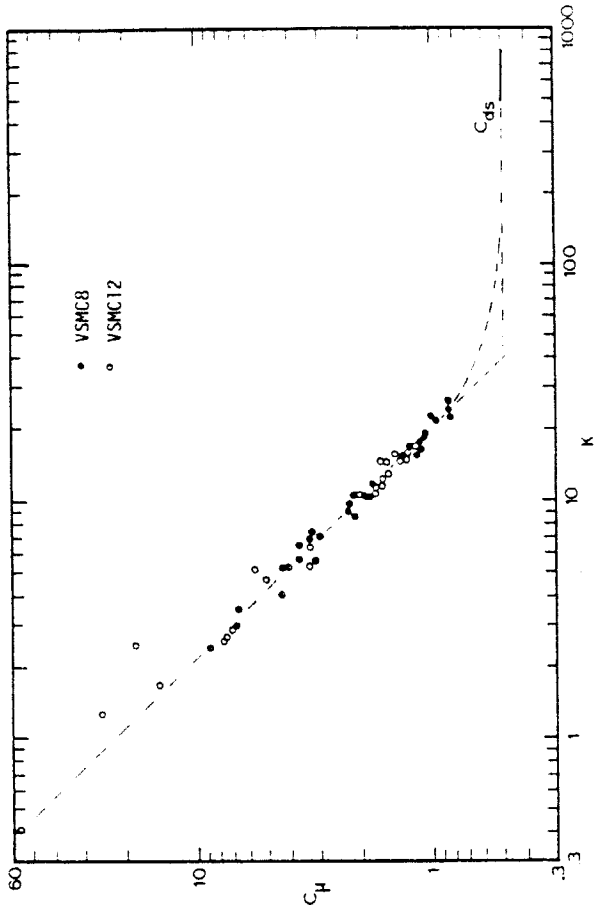

Fig. 2 Maximum force coefficient for vertical smooth cylinders

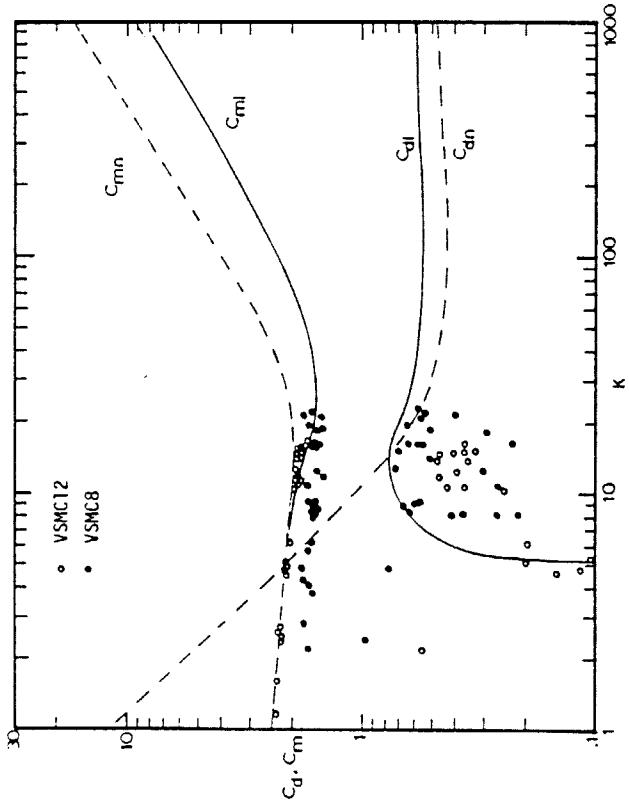

Fig. 3 Force transfer coefficient for vertical smooth cylinders

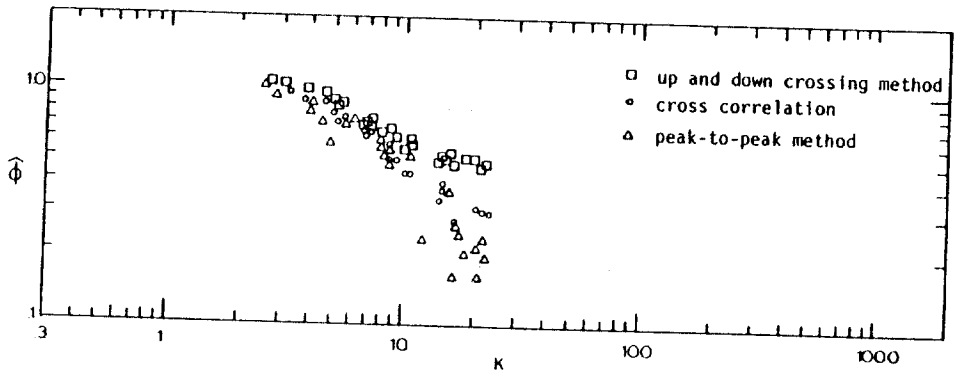

Fig. 4 Phase shift for the VSRC.02

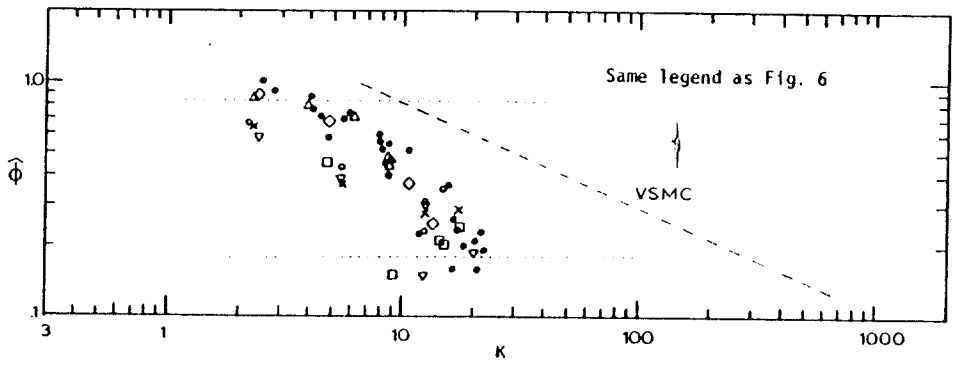

Fig. 5 Phase shift for the VSRC.02 and the AMRC using peak-to-peak method

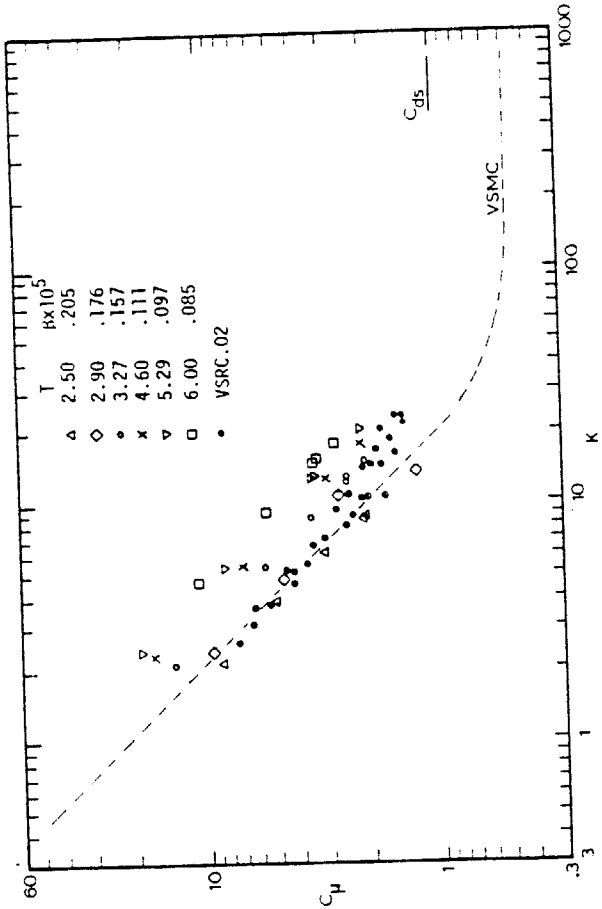

Fig. 6 Maximum force coefficient for the VSRC.02 and the AMRC using peak-to-peak method